On implementation aspects of a virtual approximation-based BEM solver for complex 3D objects in electromagnetism

Emanuele Arcese (CEA CESTA)

Joint collaboration with Thierry Hocquellet (CEA CESTA), Sébastien Pernet (ONERA)

NEMESIS-Gmsh workshop, IMAG, January 26-27, 2026

Context and motivation

Context: Analysis of time-harmonic electromagnetic (EM) scattering phenomena by a complex 3D object in radar stealth or EM compatibility applications. The object can

- be electrically large ($\lambda \ll L$, L is the object charact. size)
- consist of several homogeneous (isotropic) components of disparate sizes

Motivation: Accurate evaluation of scattered fields using boundary integral equations ➔ boundary element method (BEM) that are

- Fast (necessity of only surface mesh of the domain ➔ 2-manifolds)
- Accurate (explicit knowledge of the fundamental solution of PDE)

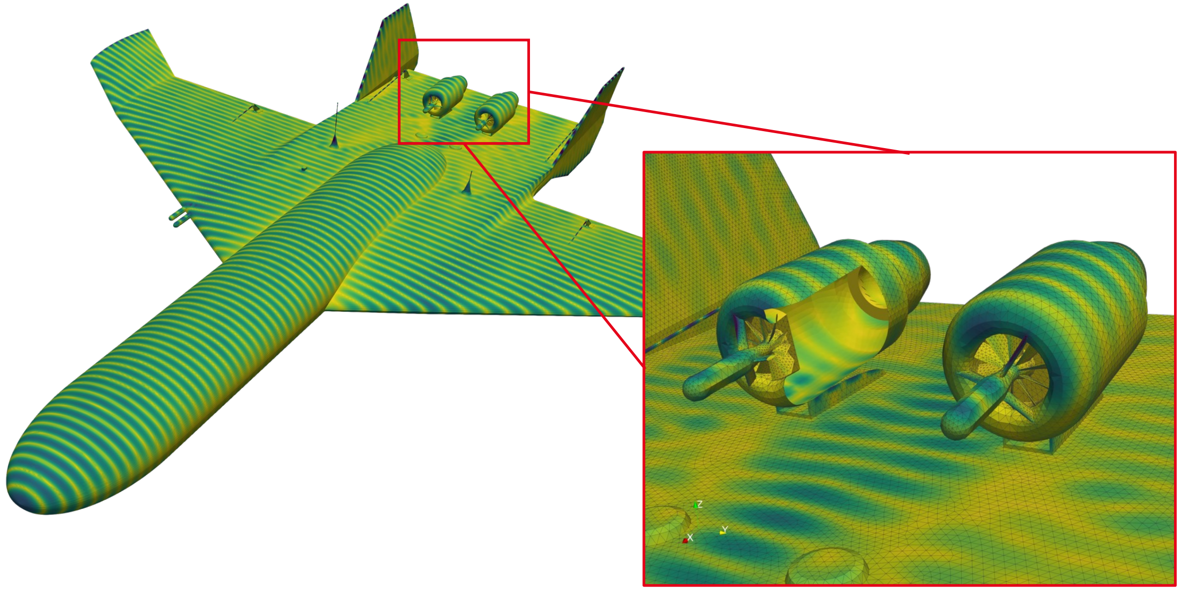

Scattering simulation of an electrically large UAV

Context and motivation

Context: Analysis of time-harmonic electromagnetic (EM) scattering phenomena by a complex 3D object in radar stealth or EM compatibility applications. The object can

- be electrically large ($\lambda \ll L$, L is the object charact. size)
- consist of several homogeneous (isotropic) components of disparate sizes

Motivation: Accurate evaluation of scattered fields using boundary integral equations ➔ boundary element method (BEM) that are

- Fast (necessity of only surface mesh of the domain ➔ 2-manifolds)
- Accurate (explicit knowledge of the fundamental solution of PDE)

➢ CEA's in-house code based on classical BEM [Augonnet et al., 2019]
  - Triangular surface meshes
  - Fast direct solution algorithms (LU, $\mathcal{H}$-matrix technique)
  - Hybrid shared-distributed parallelism

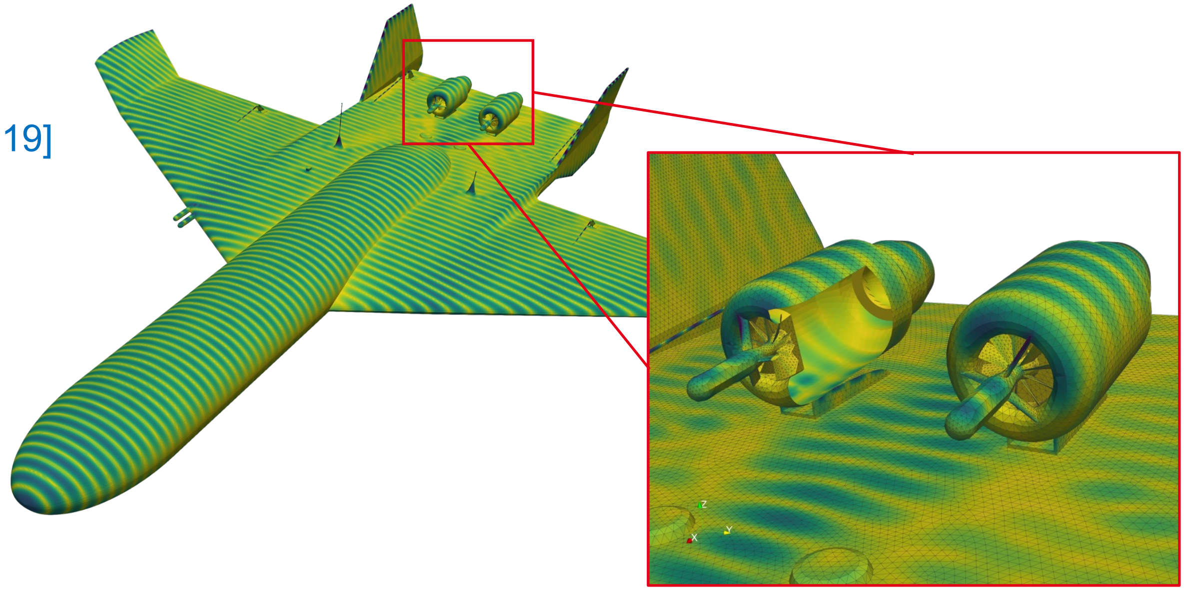

Scattering simulation of an electrically large UAV

Context and motivation

Context: Analysis of time-harmonic electromagnetic (EM) scattering phenomena by a complex 3D object in radar stealth or EM compatibility applications. The object can

- be electrically large ($\lambda \ll L$, L is the object charact. size)
- consist of several homogeneous (isotropic) components of disparate sizes

Motivation: Accurate evaluation of scattered fields using boundary integral equations ➔ boundary element method (BEM) that are

- Fast (necessity of only surface mesh of the domain ➔ 2-manifolds)
- Accurate (explicit knowledge of the fundamental solution of PDE)

Difficulty: Classical BEM are well established and adapted to HPC but …

… not robust to hanging nodes!

➢ Lack of flexibility in handling "optimal" mesh obtained e.g. by
  - Local refinement / coarsening
  - Gluing together various meshes of different densities

Complex scatterers ➔ overly dense meshes (intractable problems)

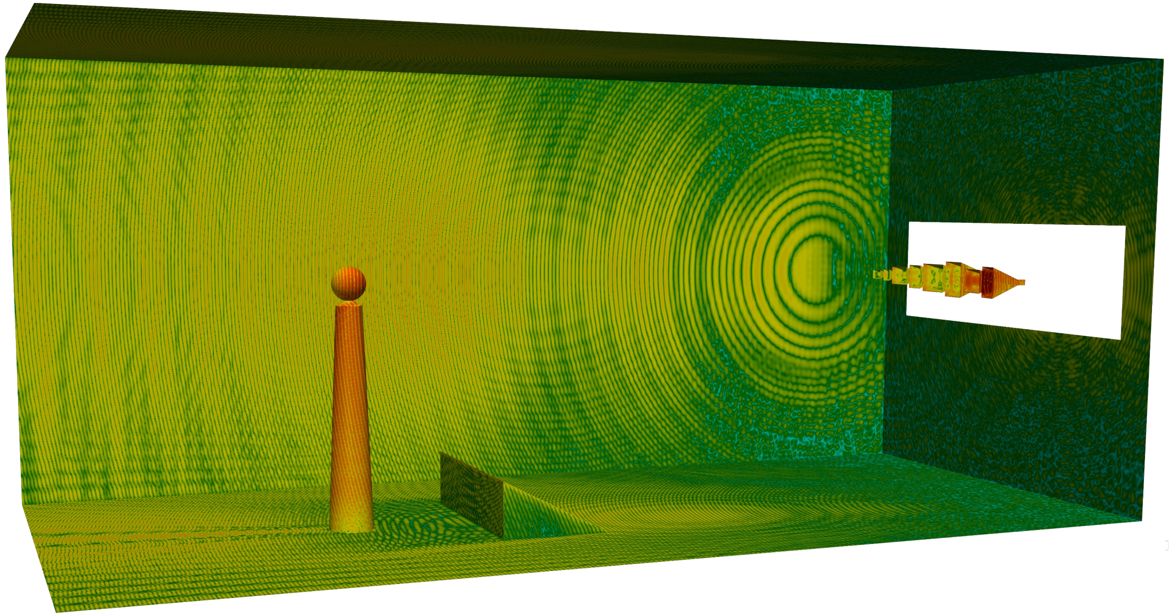

Scattering simulation of an anechoic chamber (e.g. 10M to 100M of unkn.s)

Context and motivation

Context: Analysis of time-harmonic electromagnetic (EM) scattering phenomena by a complex 3D object in radar stealth or EM compatibility applications. The object can

- be electrically large ($\lambda \ll L$, L is the object charact. size)
- consist of several homogeneous (isotropic) components of disparate sizes

Motivation: Accurate evaluation of scattered fields using boundary integral equations ➔ boundary element method (BEM) that are

- Fast (necessity of only surface mesh of the domain ➔ 2-manifolds)
- Accurate (explicit knowledge of the fundamental solution of PDE)

Difficulty: Classical BEM are well established and adapted to HPC but …

… not robust to hanging nodes!

➢ Lack of flexibility in handling "optimal" mesh obtained e.g. by
  - Local refinement / coarsening
  - Gluing together various meshes of different densities

Complex scatterers ➔ overly dense meshes (intractable problems)

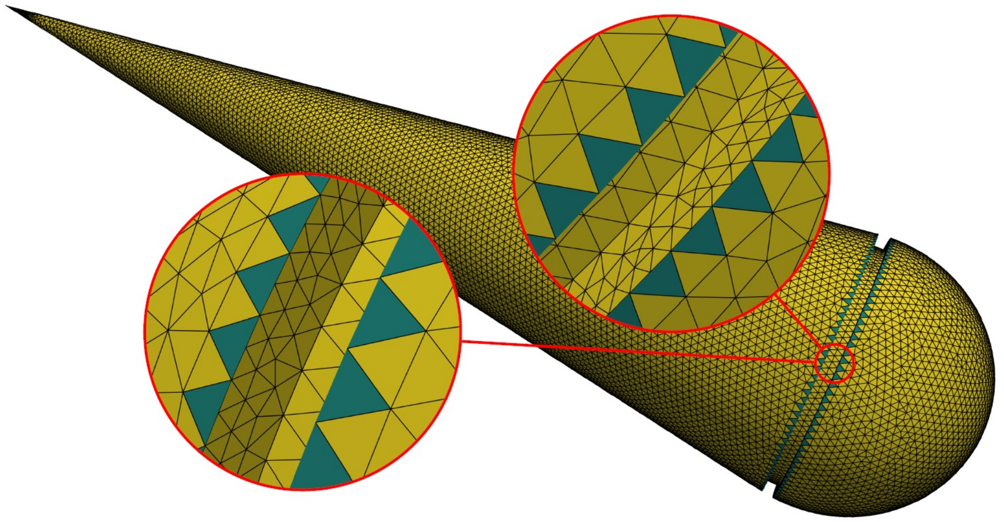

Example of polygonal mesh

A solution : Conforming approximations on general meshes ➔ Virtual element method (VEM) for BEM [Touzalin, 2025]

➢ Use of flexible polygonal meshes to capture EM details

Practical examples of EM benchmarks [1/2]

Analysis of shielding effectiveness of a metallic box with a very thin slot

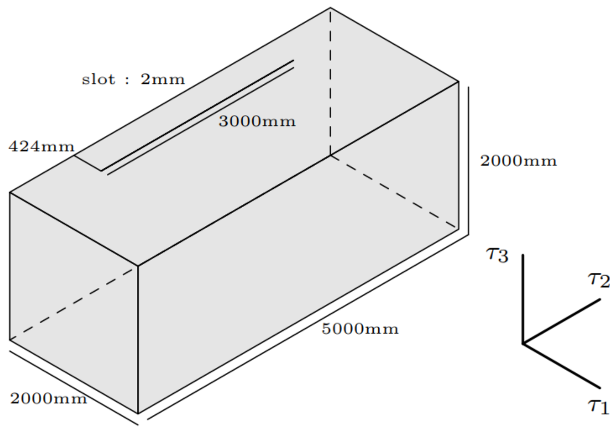

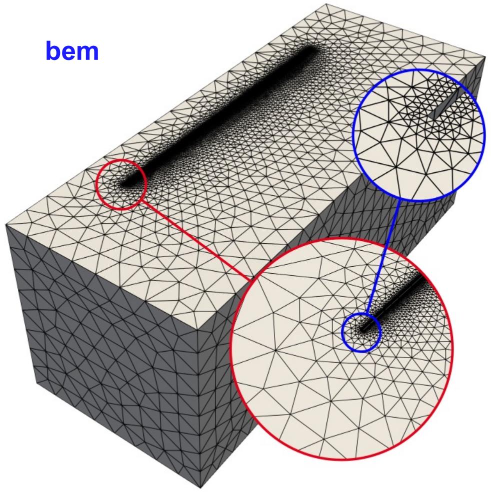

Triangular mesh for BEM

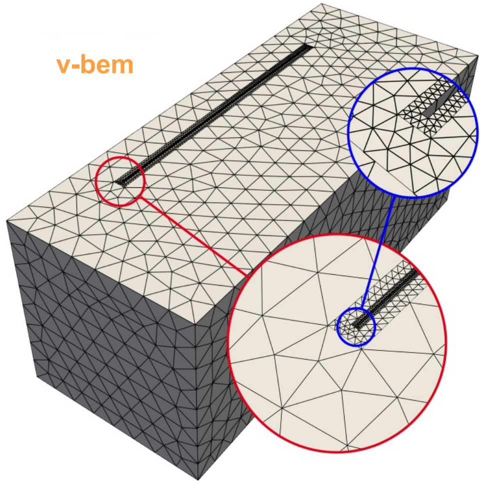

Hybrid (polygonal) mesh for V-BEM

- Accuracy and performance

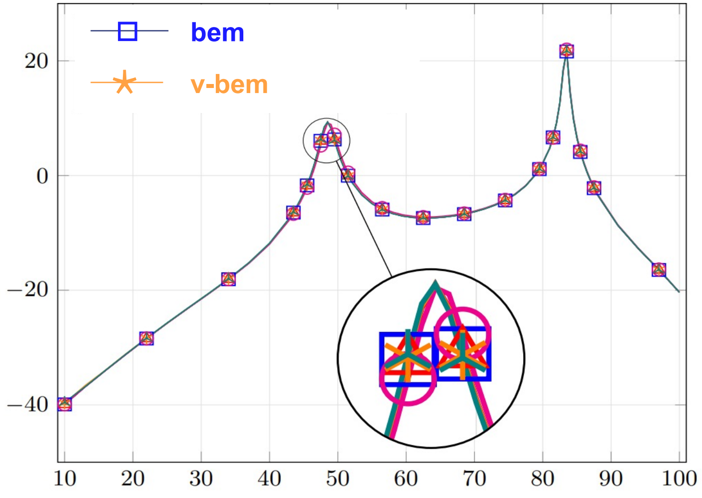

Modulus of scattered field E inside cavity (dB) vs. frequency (MHz)

Method	# unknowns	Computational cost (assembly)
BEM	64 654	813 s
V-BEM	**30 079**	**321 s**

Practical examples of EM benchmarks [2/2]

Analysis of radar signature (scattered far fields) of a metallic cone-sphere with gap

↪ The gap width is 1% of the cone-sphere length.

❑ Accuracy and performance

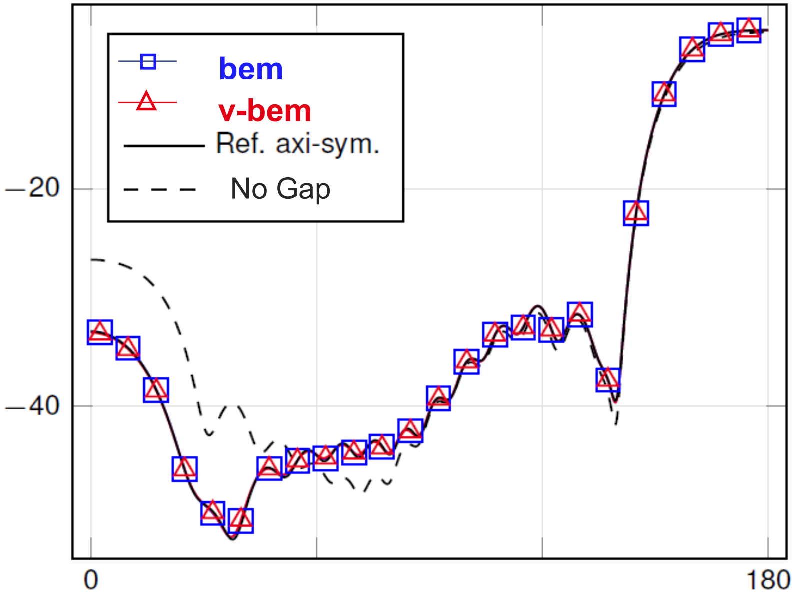

Radar signature (dB) vs. observation angle (degree)

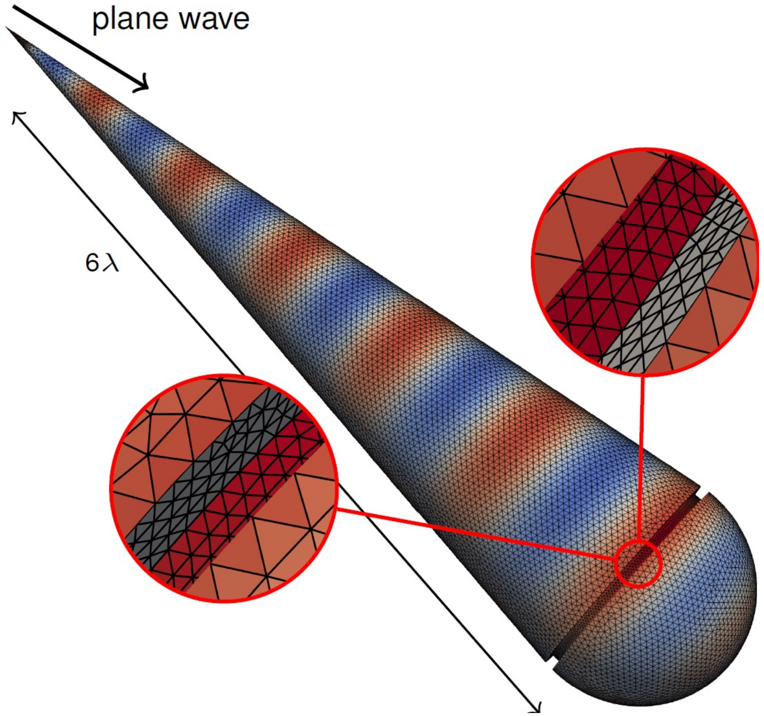

Hybrid (polygonal) mesh for V-BEM

Method	# unknowns	Computational cost (assembly)
BEM	61 662	5 160 s
V-BEM	**59 783**	**4 480 s**

MODILLON : an in-house mesh handling library

User-friendly Python API based on the Gmsh API (Gmsh model as pivot format) designed to share all in-house developments concerning the handling of classical meshes

Main goals :

- Read/Write different file formats (abaqus, I-DEAS universal, …)
- Provide mesh informations (element description, element quality, free boundary edges, …)
- Manipulate/modify meshes (extrusion of a 2D mesh, extraction mesh parts,)
- Check meshes according to code-specific criteria (orientation, mesh size, …)

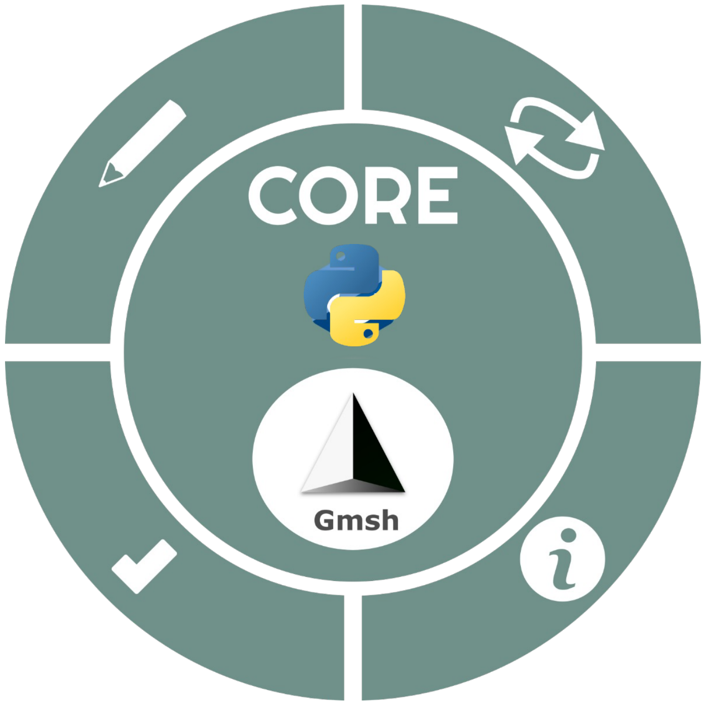

Up-to-date library can handle :

➢ Large variety of mesh formats (meshing libraries or simulation codes, in-house or commercial)

➢ Meshes with hundreds of millions of elements (triangles, quadrangles, tetrahedra, hexahedra, …)

Early strategy for the generation of meshes of flat polygons

- **Fully polygonal meshes (numerical method validation, debug purposes)**
  - Use of the open-source library Voro++ (in combination with Gmsh if needed) ➔ many mesh formats (.voro, .vtk, .vbem, .msh) !

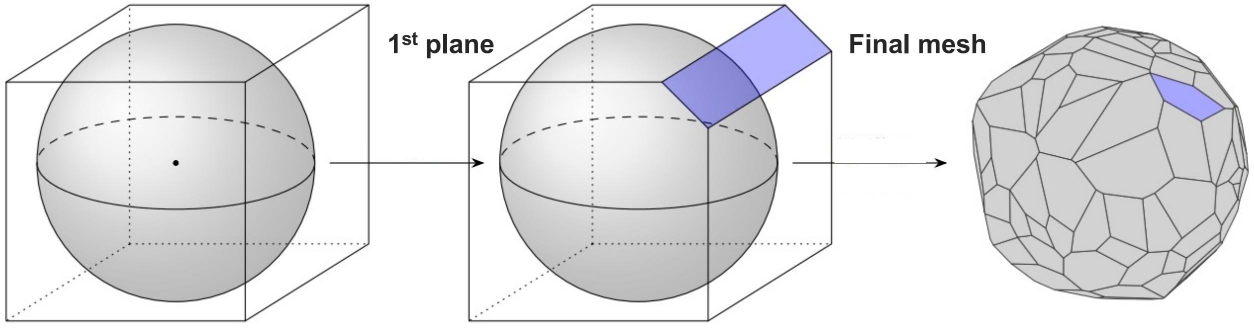

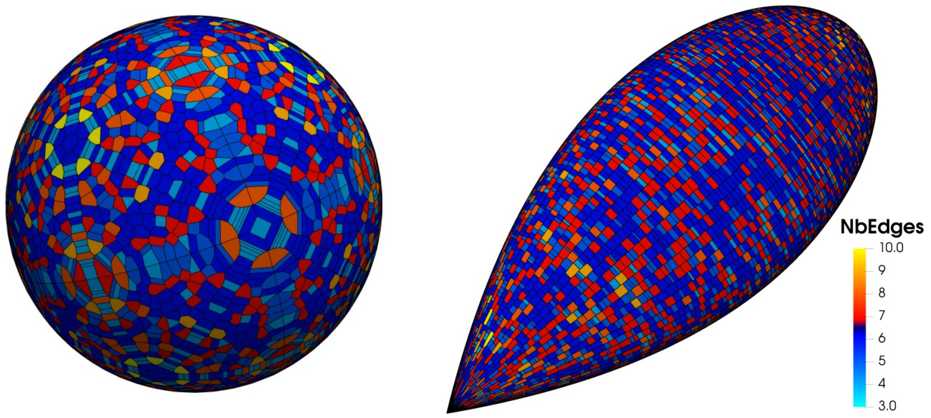

Mesh of a sphere

Mesh of the NASA almond

Early strategy for the generation of meshes of flat polygons

- **Fully polygonal meshes (numerical method validation, debug purposes)**
  - Use of the open-source library Voro++ (in combination with Gmsh if needed) ➔ many mesh formats (.voro, .vtk, .vbem, .msh) !

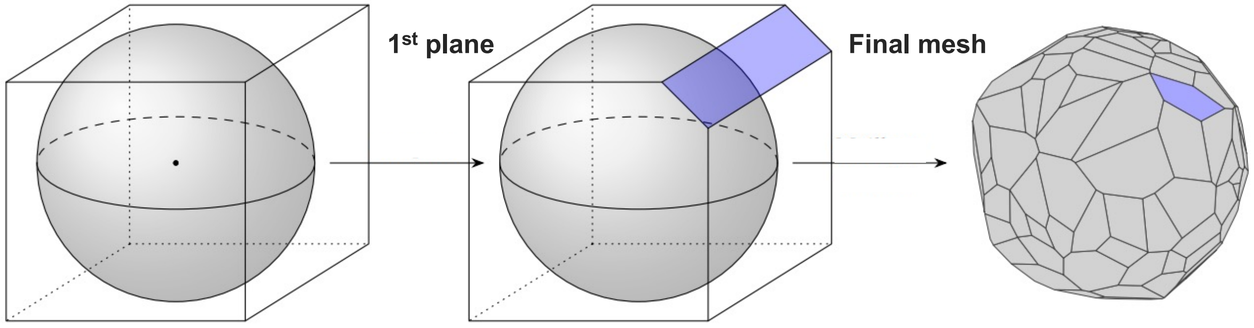

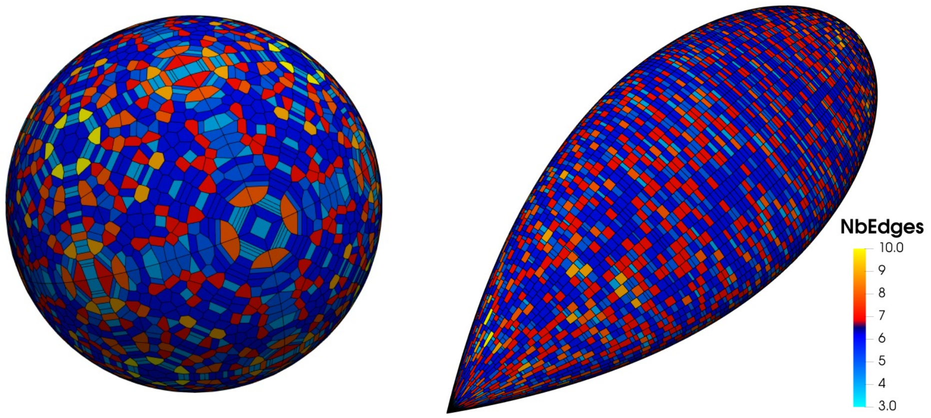

Mesh of a sphere **Mesh of the NASA almond**

- **Hybrid meshes (real-life problems)**
  - Gluing different Gmsh meshes ➔ many mesh formats (.msh, .vtk, .vbem) !

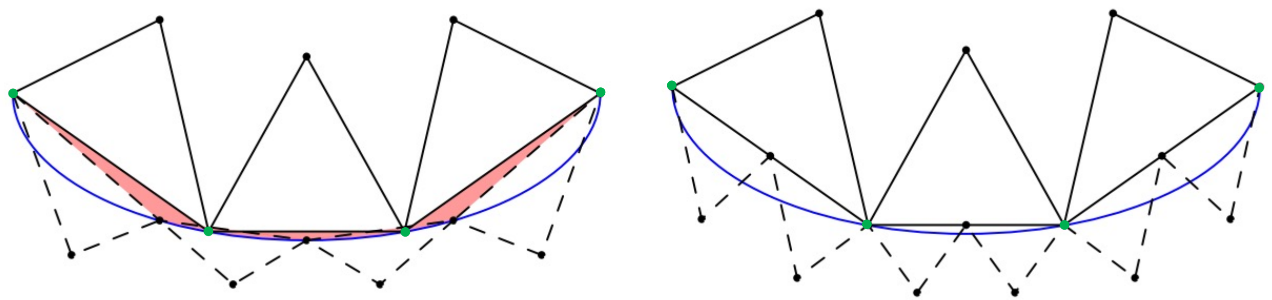

1st step : Recover the nodes of the coarser mesh at the interface

2nd step : Generate the finest mesh on the basis of the coarse nodes

➔ Dependency between coarse and fine meshes !

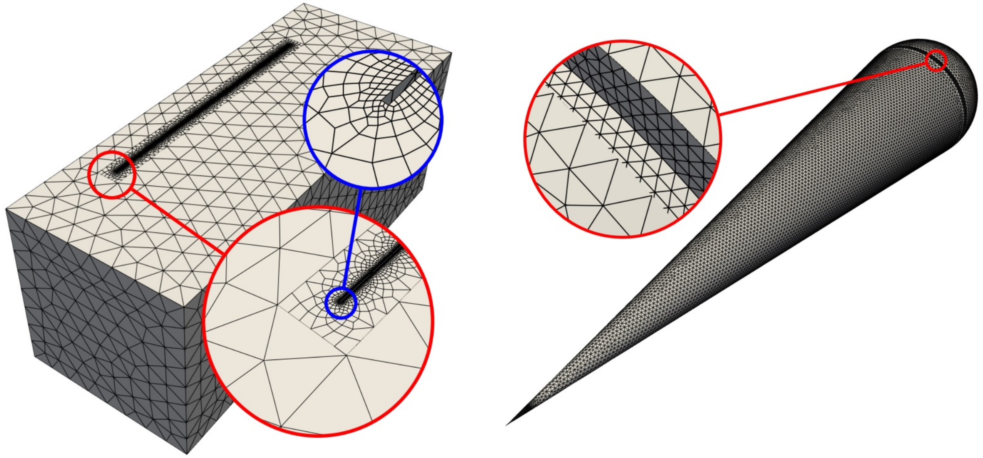

Mesh of slotted box **Mesh of a cone-sphere**

Our needs in relation to (curved) polytopal meshes

Pre-processing

- Generation of polygonal meshes via Gmsh (by dual mesh or aggregation?)
  - Taking into account polygons into mesh formats (via msh files)
  - Ability to guide the mesh generation according to a local mesh size field (as for classical elements)
  - Definition/control of the orientations of normal vectors within the mesh of each physical surface
  - What about curved polygons? (e.g. a practical approach satisfying hyp. 22 of [Droniou et al.,2025])

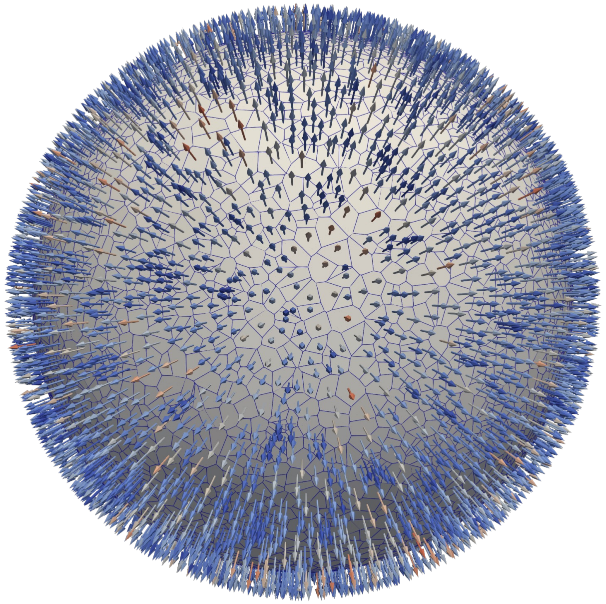

Normal vectors related to a polygonal mesh

- Check the mesh regularity via Gmsh
  - Definition of quality criteria in the context of polygons (translation of theoretical hyp.s on mesh regularity, e.g. [Sorgente et al., 2022])

Our needs in relation to (curved) polytopal meshes

- Manipulation of mesh within the code
  - Treatment of singular integrals of type $\int_K \int_L \frac{f(x,y)}{|x-y|^\alpha} dL_y dK_x$, with $\alpha = 1{,}2$

    ➔ access (via e.g. Gmsh API) to a “good” triangulation of mesh polygons (e.g. partition into a min number of triangles)

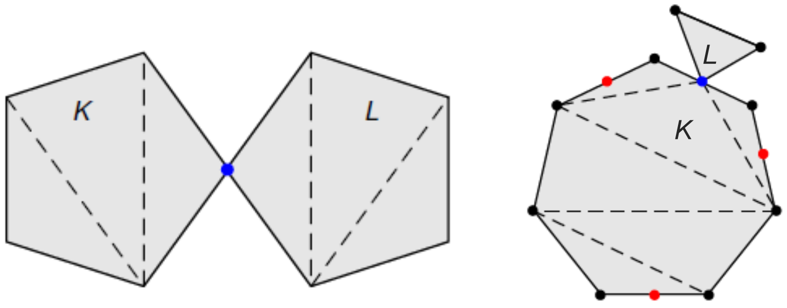

Examples of common point configurations

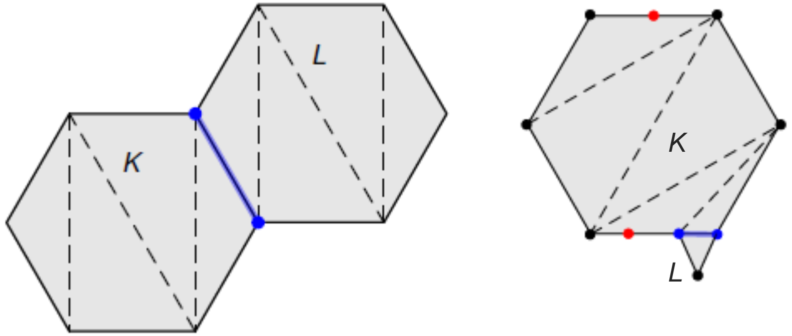

Examples of common edge configurations

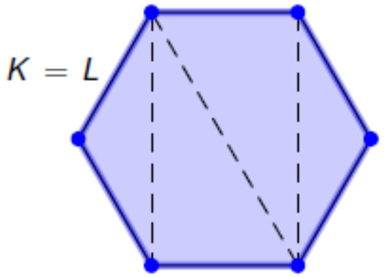

Example of identical polygons configuration

Post-processing

- Visualization via Gmsh
  - Provide exact representation of VEM projection of solution on polygons (cf. the polygon triangulation topic)

What about meshes of polyhedra ? (FEM-BEM coupling approaches, CFD applications, …)

References

Related to our work

C. Augonnet, D. Goudin, M. Kuhn, X. Lacoste, R. Namyst et P. Ramet. « A hierarchical fast direct solver for distributed memory machines with manycore nodes ». report. CEA/DAM ; Total E&P ; Université de Bordeaux, oct. 2019

A. Touzalin. « Méthode des éléments virtuels pour la discrétisation des équations intégrales de frontière en électromagnétisme dans le domaine fréquentiel ». Analyse numérique [math.NA]. ISAE-SUPAERO, 2025. Français. ⟨NNT : 2025ESAE0015⟩. ⟨tel-05149215⟩

Touzalin, E. Arcese et S. Pernet. « A boundary integral equation method based on virtual element approximation spaces for 3D electromagnetic scattering ». In : *WAVES 2024-16th International Conference on Mathematical and Numerical Aspects of Wave Propagation*. Edmond MPDL, 2024. p. 125-126.

E. Arcese, S. Pernet et A. Touzalin. « A priori error analysis of a virtual element approximation-based boundary element method for the electric field integral equation ». *Under review*. 2025.

Others

J. Droniou, M. Hanot et T. Oliynyk. « A polytopal discrete de Rham complex on manifolds, with application to the Maxwell equations ». Journal of Computational Physics, 2025, vol. 529, p. 113886.

T. Sorgente, S. Biasotti, G. Manzini et M. Spagnuolo. « The role of mesh quality and mesh quality indicators in the virtual element method ». In : Advances in Computational Mathematics 48.1, 2022, p. 3.

C. Geuzaine et J. Remacle. « Gmsh: A 3-D finite element mesh generator with built-in pre- and post-processing facilities ». In : International Journal for Numerical Methods in Engineering 79.11 (sept. 2009), p. 1309-1331

C. H. Rycroft. « VORO++: A three-dimensional Voronoi cell library in C++ ». In : Chaos : An Interdisciplinary Journal of Nonlinear Science 19.4 (déc. 2009), p. 041111

Appendix: a simple model problem

- Time-harmonic Maxwell's equations ($e^{-\iota\omega t}$)

$$\begin{cases} \mathbf{curl}\boldsymbol{E} - \iota\kappa Z_0 \boldsymbol{H} = 0 & \text{in } \mathbb{R}^3 \setminus \overline{\Omega}, \\ \mathbf{curl}\boldsymbol{H} + \iota\kappa Z_0^{-1} \boldsymbol{E} = 0 & \text{in } \mathbb{R}^3 \setminus \overline{\Omega}, \\ \boldsymbol{E} \times \boldsymbol{n} = 0 & \text{on } \Gamma, \\ \lim_{|\boldsymbol{x}|\to+\infty} |\boldsymbol{x}| \left(Z_0(\boldsymbol{H} - \boldsymbol{H}^I)(\boldsymbol{x}) \times \frac{\boldsymbol{x}}{|\boldsymbol{x}|} - (\boldsymbol{E} - \boldsymbol{E}^I)(\boldsymbol{x}) \right) = 0 \end{cases}$$

- Weak formulation of the electric field integral equation

Find $\boldsymbol{J} \in \boldsymbol{X} = \boldsymbol{H}^{-1/2}(div_\Gamma, \Gamma)$, such that, $\kappa > 0$:

$$a(\boldsymbol{J}, \boldsymbol{J}') = f(\boldsymbol{J}'), \qquad \forall \boldsymbol{J}' \in \boldsymbol{X}.$$

↪ $a(\boldsymbol{J}, \boldsymbol{J}') = \int_\Gamma \int_\Gamma G_\kappa(\boldsymbol{x}-\boldsymbol{y}) \boldsymbol{J}(\boldsymbol{y}) \cdot \boldsymbol{J}'(\boldsymbol{x}) d\gamma_y d\gamma_x - \frac{1}{\kappa^2} \int_\Gamma \int_\Gamma G_\kappa(\boldsymbol{x}-\boldsymbol{y}) div_\Gamma(\boldsymbol{J}(\boldsymbol{y}))\, div_\Gamma(\boldsymbol{J}'(\boldsymbol{x})) d\gamma_y d\gamma_x,$

↪ $f(\boldsymbol{J}') = \frac{\iota}{\kappa Z_0} \int_\Gamma \pi_t \boldsymbol{E}^I(\boldsymbol{x}) \cdot \boldsymbol{J}'(\boldsymbol{x}) d\gamma_x,$ with $G_\kappa(\boldsymbol{x}-\boldsymbol{y}) = \frac{e^{\iota\kappa|\boldsymbol{x}-\boldsymbol{y}|}}{4\pi|\boldsymbol{x}-\boldsymbol{y}|}, \qquad \boldsymbol{x} \neq \boldsymbol{y}.$

- Galerkin discretization using Raviart-Thomas finite elements (BEM)

Find $\boldsymbol{J}_h \in \boldsymbol{X}_h \subset \boldsymbol{H}(div_\Gamma, \Gamma)$, such that :

$$a(\boldsymbol{J}_h, \boldsymbol{J}'_h) = f(\boldsymbol{J}'_h), \qquad \forall \boldsymbol{J}'_h \in \boldsymbol{X}_h$$

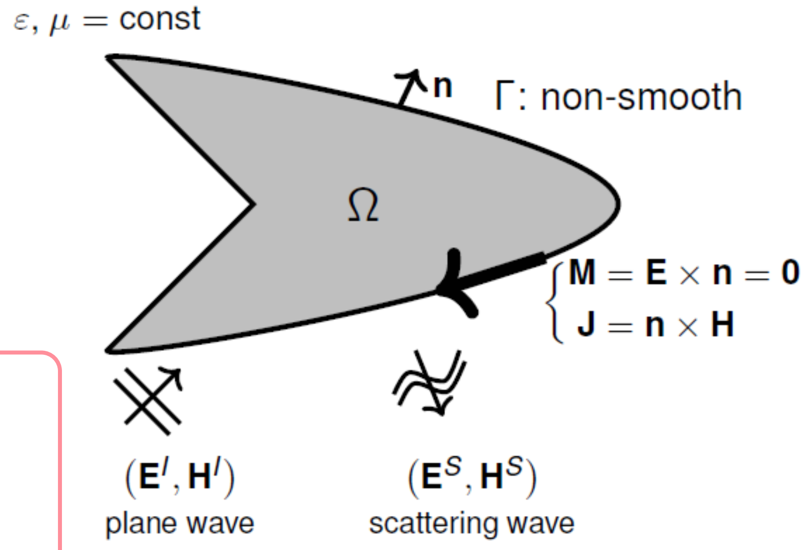

Appendix: a simple model problem

- Time-harmonic Maxwell's equations ($e^{-\iota\omega t}$)

$$\begin{cases} \mathrm{curl}\boldsymbol{E} - \iota\kappa Z_0 \boldsymbol{H} &= 0 \quad \text{in } \mathbb{R}^3 \setminus \overline{\Omega}, \\ \mathrm{curl}\boldsymbol{H} + \iota\kappa Z_0^{-1} \boldsymbol{E} &= 0 \quad \text{in } \mathbb{R}^3 \setminus \overline{\Omega}, \\ \boldsymbol{E} \times \boldsymbol{n} &= 0 \quad \text{on } \Gamma, \\ \lim_{|\boldsymbol{x}| \to +\infty} |\boldsymbol{x}| \left(Z_0(\boldsymbol{H} - \boldsymbol{H}^I)(\boldsymbol{x}) \times \frac{\boldsymbol{x}}{|\boldsymbol{x}|} - (\boldsymbol{E} - \boldsymbol{E}^I)(\boldsymbol{x}) \right) = 0 \end{cases}$$

- Weak formulation of the electric field integral equation

Find $\boldsymbol{J} \in \boldsymbol{X} = \boldsymbol{H}^{-1/2}(div_\Gamma, \Gamma)$, such that, $\kappa > 0$:

$$a(\boldsymbol{J}, \boldsymbol{J}') = f(\boldsymbol{J}'), \qquad \forall \boldsymbol{J}' \in \boldsymbol{X}.$$

$$\hookrightarrow \quad a(\boldsymbol{J}, \boldsymbol{J}') = \int_\Gamma \int_\Gamma G_\kappa(\boldsymbol{x} - \boldsymbol{y}) \boldsymbol{J}(\boldsymbol{y}) \cdot \boldsymbol{J}'(\boldsymbol{x}) d\gamma_y d\gamma_x - \frac{1}{\kappa^2} \int_\Gamma \int_\Gamma G_\kappa(\boldsymbol{x} - \boldsymbol{y}) div_\Gamma(\boldsymbol{J}(\boldsymbol{y}))\, div_\Gamma(\boldsymbol{J}'(\boldsymbol{x})) d\gamma_y d\gamma_x,$$

$$\hookrightarrow \quad f(\boldsymbol{J}') = \frac{\iota}{\kappa Z_0} \int_\Gamma \pi_t \boldsymbol{E}^I(\boldsymbol{x}) \cdot \boldsymbol{J}'(\boldsymbol{x}) d\gamma_x, \quad \text{with} \quad G_\kappa(\boldsymbol{x} - \boldsymbol{y}) = \frac{e^{\iota\kappa|\boldsymbol{x}-\boldsymbol{y}|}}{4\pi|\boldsymbol{x}-\boldsymbol{y}|}, \quad \boldsymbol{x} \neq \boldsymbol{y}.$$

- Galerkin discretization using virtual elements (V-BEM)

Find $\boldsymbol{J}_h \in \boldsymbol{V}_h \subset \boldsymbol{H}(div_\Gamma, \Gamma)$, such that :

$$a_h(\boldsymbol{J}_h, \boldsymbol{J}_h') = f_h(\boldsymbol{J}_h'), \qquad \forall \boldsymbol{J}_h' \in \boldsymbol{V}_h$$